
Model Diffusion for Certifiable Few-shot Transfer Learning

Fady Rezk^{1,2,*}, Royson Lee², Henry Gouk¹, Timothy Hospedales^{1,2}, Minyoung Kim²

¹ School of Informatics, University of Edinburgh,

² Samsung AI Center, Cambridge

Abstract

In contemporary deep learning, a prevalent and effective workflow for solving low-data problems is adapting powerful pre-trained foundation models (FMs) to new tasks via parameter-efficient fine-tuning (PEFT). However, while empirically effective, the resulting solutions lack generalisation guarantees to certify their accuracy - which may be required for ethical or legal reasons prior to deployment in high-importance applications. In this paper we develop a novel transfer learning approach that is designed to facilitate non-vacuous learning theoretic generalisation guarantees for downstream tasks, even in the low-shot regime. Specifically, we first use upstream tasks to train a *distribution over PEFT parameters*. We then learn the downstream task by a *sample-and-evaluate* procedure – sampling plausible PEFTs from the trained diffusion model and selecting the one with the highest likelihood on the downstream data. Crucially, this confines our model hypothesis to a *finite* set of PEFT samples. In contrast to the typical continuous hypothesis spaces of neural network weights, this facilitates tighter risk certificates. We instantiate our bound and show non-trivial generalization guarantees compared to existing learning approaches which lead to vacuous bounds in the low-shot regime.

1 Introduction

Generalisation certificates are crucial for high-importance applications where accuracy should be guaranteed for legal or ethical reasons. Guarantees should certify the minimum testing accuracy expected on unseen data drawn from the training distribution. However, it is hard to establish non-trivial guarantees for large neural networks, since large learning capacity tends to produce looser guarantees. As such, there have only been a few successful demonstrations of non-vacuous guarantees for contemporary neural networks, even in the large-data regime [7, 21, 15].

What about learning with sparse rather than large data? The problem of low-data learning is highly topical, due to the plethora of important limited-data applications [36], but challenging due to the difficulty of learning a large number neural network parameters without overfitting. This need has inspired several lines of research that make use of different forms of knowledge transfer, including meta-learning [10] and parameter-efficient transfer learning (PEFT) [11] from foundation models. While PEFT methods have recently been more empirically effective, neither family of approach has produced methods that can provide low-shot generalisation guarantees, to our knowledge. From a learning theoretic perspective this is because existing algorithms still search a hypothesis space (e.g., all neural network weights $\theta \in \mathcal{R}^N$) large enough to make known bounds vacuous when instantiated.

This paper introduces a novel approach to knowledge transfer that ultimately learns downstream tasks by *picking from a finite set of hypothesis*, where the set of hypothesis is fit to the upstream tasks. Our method, STEEL (Sample ThEn Evaluate Learner), facilitates using classic finite-hypothesis bounds, which are simple and tight, but not typically used in contemporary machine learning – which focuses on learning continuous value neural network parameters.

*Correspondence to Fady Rezk <s1985200@ed.ac.uk>

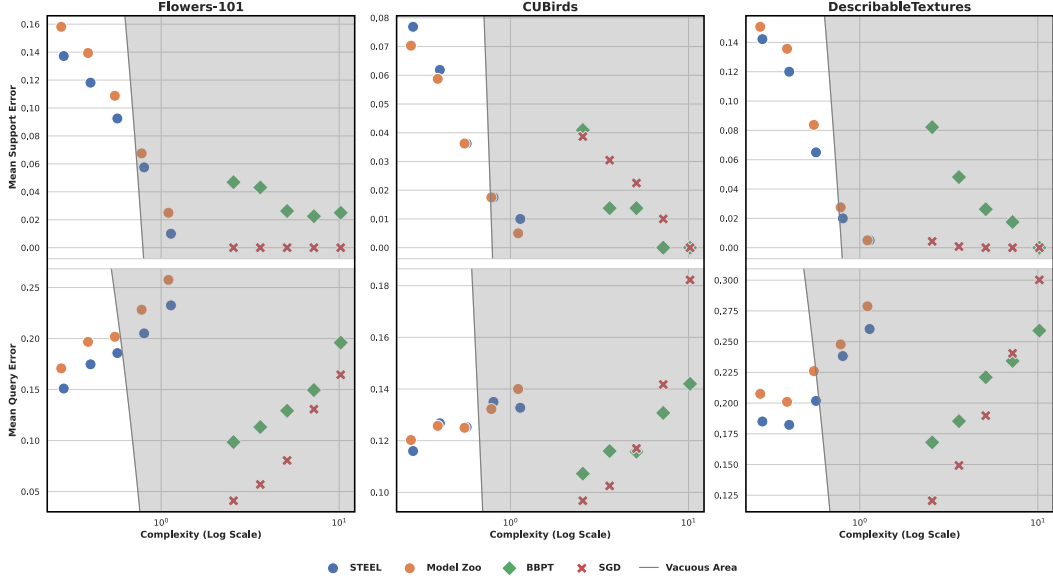


Figure 1: Generalization bounds for adapting CLIP to novel tasks (5-way classification with 1–16 examples per class). Plots show classification error (y-axis) versus the complexity term (x-axis, log scale; square root terms from Equations 3, and 7). Top/Bottom: Mean support/query (train/test) error on new tasks. Shaded regions indicate vacuous bounds, where $(\text{support error} + \text{complexity}) \geq 1$. Non-vacuous guarantees lie in the unshaded region. Competing methods (SGD, BBPT) fail to achieve non-vacuous bounds. In contrast, our method yields non-vacuous guarantees without significantly compromising training fit (top) or test accuracy (bottom).

More specifically, in the upstream phase, we fit PEFT modules to available source tasks, and then train a parameter diffusion model to generate PEFTs according to this task distribution. In the downstream phase, we learn by sample-then-evaluate instead of traditional gradient descent. PEFT modules, unconditionally generated by the diffusion model, are scored using the target task training set, and learning is to choose the highest scoring module. Compared to the original set of upstream models, the diffusion model can be more compact, and can interpolate between the original model set to achieve higher accuracy. This procedure is gradient-free, which has some scalability benefits [17, 23], but more importantly it facilitates the use of PAC-Bayes finite-hypothesis bounds to provide non-vacuous guarantees, all while maintaining similar empirical accuracy to mainstream few-shot learning approaches. Figure 1 shows some illustrative results, demonstrating our learner’s ability to maintain practical efficacy while being constrained to low enough complexity to provide non-vacuous guarantees (white zone).

In summary, our contributions are: (1) Introducing a novel learning paradigm for gradient-free transfer learning designed to facilitate accuracy guarantees for downstream tasks, even in the low-shot regime. (2) The first practical demonstration of non-vacuous generalization bounds for low-shot learning in large language and vision architectures.

2 Risk Certificates for Deep Models

Certifying model generalization performance is fundamental in theoretical machine learning [32, 26, 19]. Vapnik–Chervonenkis (VC), Rademacher, and PAC-Bayes bounds connect empirical risk (computable) to generalization risk (impossible to compute) through inequalities. Here we discuss the core concepts of risk certificates and why they are challenging to apply to deep models.

Let $h \in \mathcal{H}$ be a hypothesis (prediction function $y = h(x)$) and \mathcal{H} the hypothesis space. In deep learning, h corresponds to a model with parameters θ , and $\Theta (\ni \theta)$ represents all possible parameter values, serving as the hypothesis space. A learning algorithm (i.e., SGD) selects θ from Θ given empirical data $S = (x_i, y_i)_{i=1}^n$ sampled i.i.d. from distribution T . The goal is minimizing generalization risk $R(\theta) = \mathbb{E}_{(x,y) \sim T} [l(\theta; x, y)]$, where $l(\theta; x, y)$ is the instance risk. Since computing $R(\theta)$ is impossible without access to T , we minimize empirical risk $r(\theta) = \frac{1}{n} \sum_{(x,y) \in S} l(\theta; x, y)$.

Nevertheless, $r(\theta)$ is a surrogate for $R(\theta)$ and does not give any certificate about true generalization risk. Therefore, theoretical bounds relate R and r as follows. For any $\theta \in \Theta$:

$$R(\theta) \leq r(\theta) + \text{ComplexityTerm}(\dim(\Theta), n) \quad (1)$$

where the complexity term depends on data size n and hypothesis space complexity $\dim(\Theta)$, decreasing as n increases and $\dim(\Theta)$ decreases². The right side of (1) is the risk certificate, which guarantees an upper bound on the risk of generalization. All terms on the right side are also computable. Different bounding methods, for example VC and Pac-Bayes bounds, produce different complexity terms. In totality, certificates above 1 (with $l \in [0, 1]$) are vacuous, while we refer to those below 1 (or sometimes less than the random guess risk in the classification setting) as non-vacuous.

Traditional models like linear SVM achieve non-vacuous bounds through proper regularization [32, 26]. However, conventional deep neural networks trained by gradient descent lack non-vacuous bounds unless n is extremely large, due to high $\dim(\Theta)$ from numerous *continuous* parameters. Even sparse adapter methods (e.g., LoRA [11], LoRA-XS [3]) face challenges from the continuous nature of Θ . No existing deep learning approach achieves meaningful generalization bounds in low-shot settings.

3 Proposed Approach

3.1 Our Approach at High Level

We propose a novel approach using a *finite* hypothesis space and gradient-free learning, departing from traditional continuous methods. In multi-task transfer learning, we learn a task distribution via a diffusion generative model, creating a *finite* hypothesis space Θ from model-generated samples. Our simple learning algorithm selects the $\theta \in \Theta$ with minimal empirical risk, using heuristic search for efficiency with large Θ to reduce the forward-pass overhead (as detailed in Sec. 3).

This approach, combined with finite-hypothesis PAC-Bayes bounds, yields tight non-vacuous risk certificates on large-scale LLM/vision benchmarks using FLAN-T5/CLIP models. Importantly, test performance remains comparable to standard learning algorithms. The *evaluate-then-select* strategy optimizes PAC-Bayes bounds by keeping the complexity term constant. We present the formal problem setup below before detailing our approach in Sec. 3.3.

3.2 Problem Setup and Notation

We describe the *low-shot cross-task transfer learning* problem that we aim to solve in the paper. Consider that we have a training pool of *related* tasks T_1, \dots, T_N , i.i.d. sampled from some unknown but true task distribution $p_{true}(T)$. At test time, we are given a new test task T^* sampled from the same $p_{true}(T)$, but only in the form of low-shot data samples $S^* = \{(x_i, y_i)\}_{i=1}^n$ (aka support data) from T^* . By low shot, we mean the number of support samples n is small. We remark that in terms of problem specification and assumptions, this is almost exactly the same as assumed by both the meta-learning [10] and model-zoo [12] literature.

Our goal is to find a way to ensure tight generalization bounds for the underlying deep models at test time. As discussed in Sec. 2, a main challenge here is that we have low-shot data S^* and a large number of model parameters, where the latter immediately translates into high hypothesis space complexity. Hence, applying the traditional learning theories directly to this problem leads to vacuous error bounds. We come up with a new method that exploits the training tasks to transfer the knowledge to unseen tasks so that it can offer tight non-vacuous risk certificates.

3.3 Transfer Learning by Sampling and Evaluation

Our first observation is that gradient-based model adaptation to low-shot samples S^* must be avoided to reduce hypothesis space complexity (Sec. 2). Our key intuition is that we can learn the task

²In the PAC-Bayes bounds, the risks are measured as expected risks over some (posterior) distribution over θ rather than point estimates. Also the complexity term is expressed in terms of divergence from a prior distribution. But if we confine the posterior to be sharply concentrated at a single point θ and use a flat prior, this roughly follows the form of (1). Also certain PAC-Bayes bounds have nonlinear relation between R and r , however, they can be approximated as (1), where this simplification does not affect the reasoning in our paper.

distribution $p_{true}(T)$ from training tasks $\{T_i\}_{i=1}^N$, but doing so introduces a strong inductive bias or regularization. Let θ_i be the learned neural network parameters for task T_i . (Throughout, we treat PEFT adapter parameters as θ , keeping the pre-trained backbone fixed.) We view θ_i as the best description of T_i and collect task-wise parameters $\{\theta_i\}_{i=1}^N$. Learning $p_{true}(T)$ thus reduces to a *density estimation problem*, i.e., estimating $p(\theta)$ from i.i.d. samples $\{\theta_i\}_{i=1}^N$, treating $p(\theta)$ as a surrogate for $p_{true}(T)$.

We learn a diffusion model $p(\theta)$ with $\{\theta_i\}_{i=1}^N$ as training data following Ho et al. [8]. At test time, the estimated $p(\theta)$ serves as a proxy for $p_{true}(T)$. We generate plausible candidate samples θ (i.e., tasks T) and select the one closest to T^* . Since only S^* of T^* is available, we choose the sample with the least discrepancy from S^* via the minimum loss rule: $\arg \min_{\theta \in \Theta} \sum_{(x,y) \in S^*} l(\theta; x, y)$, where Θ is the set of diffusion model candidates. This corresponds to empirical risk minimization where Θ acts as the *hypothesis space*, and we this learner STEEL (Sample ThEn Evaluate Learner).

This strategy amounts to *selection from a finite hypothesis space*, rather than searching a continuous space via gradient-based fine-tuning. The choice of a finite hypothesis set (diffusion model samples) before learning enables a strong regularizing inductive bias learned from upstream tasks.

3.4 Risk Certificate with Finite Hypothesis Space

Suppose we have a well-trained zoo of (PEFT adapter) parameters $\bar{\Theta} = \{\theta_i\}_{i=1}^N$, where each θ_i is the optimal parameters for the i -th training task ($i = 1, \dots, N$). Without the diffusion training with $\bar{\Theta}$, nothing can prevent us from using the the model zoo $\bar{\Theta}$ itself as our hypothesis space, i.e., $\Theta = \bar{\Theta}$. This becomes more reasonable as N goes larger since $\bar{\Theta}$ would be richer and closer to the true $p_{true}(T)$. We will call this strategy of $\Theta = \bar{\Theta}$ the *model zoo* strategy. To go beyond this, our full STEEL method trains a diffusion model $p(\theta)$ with $\bar{\Theta}$, and builds Θ using the samples from it³. Whereas both are our proposals, the diffusion is our main strategy as it is more attractive in the following aspects: i) the model zoo strategy requires a large amount of space to store the N models while the diffusion strategy is more scalable, only needing to store the diffusion model itself; ii) The diffusion model is widely known to have strong interpolation capability to approximate the target density better, which in practice can provide improved test accuracy

Few-shot adaptation is done by evaluate-then-select:

$$\theta^* = \arg \min_{\theta \in \Theta} r(\theta) = \frac{1}{n} \sum_{(x,y) \in S^*} l(\theta; x, y) \quad (2)$$

We expect that Θ is rich enough to represent the true task distribution $p_{true}(T)$ faithfully, and the adapted (“selected”) θ^* will generalize well on unseen samples from T^* .

A crucial benefit of our test-time adaptation strategy (2) is that we have a tight provable generalization error bound that can serve as a risk certificate for its test-time prediction quality. This mainly originates from the *finite* hypothesis space Θ . More specifically, using the PAC-Bayes theorems (e.g., Sec. 2.1.3 in [1]), we can show that with probability at least $1 - \epsilon$,

$$R(\theta) \leq r(\theta) + C \cdot \sqrt{\frac{\log \frac{|\Theta|}{\epsilon}}{2n}} \quad \text{for any } \theta \in \Theta \quad (3)$$

where $R(\theta) = \mathbb{E}_{(x,y) \sim T^*} [l(\theta; x, y)]$ is the generalization error of θ , and C is the maximal loss value (i.e., $0 \leq l \leq C$). The bound immediately comes from the PAC-Bayes theorem with the (data-independent) uniform prior over Θ and the Dirac’s delta posterior choice. Since the size of the hypothesis space $|\Theta|$ only appears in the log term, a massively large Θ is allowable while retaining a tight bound. Furthermore, the bound can be minimized with the smallest empirical error $r(\theta)$, i.e., $\theta = \theta^*$, which justifies our evaluate-then-select strategy (2).

However, the computational question naturally arises: *How do we solve (2) efficiently?* We consider two solutions:

³Alternatively, we can union model zoo and diffusion samples together to build a larger hypothesis space. This is practically effective, but in this paper we focus only on model zoo and diffusion strategies so as to contrast their behaviors more carefully.

- **Exhaustive search.** We go through every θ in Θ , evaluate the loss $r(\theta)$, and choose the minimum one. Even though we guarantee to find θ^* always with the minimal empirical $r(\theta)$, this is computationally very expensive (often intractable for the LLM cases due to prohibitive $|\Theta|$ forward passes or text generation).
- **Hierarchical search.** This is the well-known tree search strategy to find an approximate solution. For instance, we can do hierarchical clustering of θ s in Θ , evaluate the losses of the top level clusters (either cluster centroids or medoids), and choose the best cluster. Then we focus only on the θ s that belong to the selected cluster, discarding the rest, and go on recursively. This may find a good approximate solution θ close to θ^* in $O(\log |\Theta|)$ time. However, we may possibly end up with suboptimal (underfit) empirical error $r(\theta)$.

We emphasize again that in all these strategies, the generalization error bound (3) holds true, but with possibly differently/suboptimally selected θ s in the latter case, which may imply (slight) increase in the empirical loss $r(\theta)$, and hence a slight loosening of the obtained certificate.

4 Related Work

Risk certificates. While traditionally applied to simple models, recent work extends risk certificates to deep learning. Notable approaches include using data-dependent priors [21] and parameter quantization of PEFT adapters [15] in tabula-rasa and single source transfer learning respectively. Nevertheless, these still require large training sets to obtain non-vacuous bounds. In the meta-learning literature, Zakerinia et al. [39] proposed meta-learning PAC-Bayes bounds, which aims to facilitate tighter generalisation bounds by extracting a common prior from up-stream tasks in a multi-task setting. However, it was only demonstrated on toy problems and doesn't scale to large models due to the memory requirements of nested gradient computations.

Model diffusion methods. Several works explore diffusion for generating model parameters: NNDiffusion [35] for BN modules, ProtoDiff [6] for ProtoNet-based few-shot learning, and MetaDiff [40] and D2NWG [28] for gradient-free meta-learning. Scaling properties of Diffusion based learning were also explored [25]. However, none provide risk certificates for the generated models.

Sparse adapter (PEFT) methods. Sparse adapters reduce learnable parameters, crucial for our diffusion-based sampling. While LoRA [11] uses trainable low-rank matrices and VeRA [13] uses fixed matrices with trainable diagonals, we adopt LoRA-XS [3], which uses SVD with a trainable full matrix for the singular values. Such adapters have facilitated large-data guarantees [15], but in our framework they will facilitate low-shot guarantees.

Connection to our Approach. In terms of assumptions, we consider the same multi-task setting of meta-learning [10], model-zoo [12] and model diffusion [35] approaches. They all aim to facilitate downstream learning by knowledge transfer from upstream tasks. In terms of solution we share the benefit of model-zoo and model-diffusion methods in being able to use third-party off-the-shelf pre-trained upstream models, rather than requiring an expensive joint learning procedure like meta-learners. Like meta-learners and model-diffusers, but unlike zoo methods, we do learn a task-agnostic component (the diffusion model).

5 Experiments

Metrics for Certified Learning Quality: In the low-shot learning context, we run many learning episodes with different random small training sets [36]. Thus we need evaluation metrics for the typical empirical performance and certificate strength instead of a single accuracy and certificate for one large scale learning [15]. This is straightforward for empirical test performance: we report the average over episodes of the relevant task metric (e.g., accuracy, RMSE). For certificates, we report the minimum (best), median (typical) and maximum (worst) case error guarantee over all downstream tasks. Since many learners often produce vacuous certificates in the low-shot regime (e.g., guaranteed error not below 1), we use *the proportion of tasks which have a non-vacuous certificate* as our leading metric. Finally, to quantify how tight the certificates are, we also report *gap* - the average distance between certificates and query errors over all faithful bounds. More concretely, this is computed as $\sum_{i=0}^K \frac{\max(0, \text{bound}_i - \text{query error}_i)}{K}$ where K is the total number of downstream tasks.

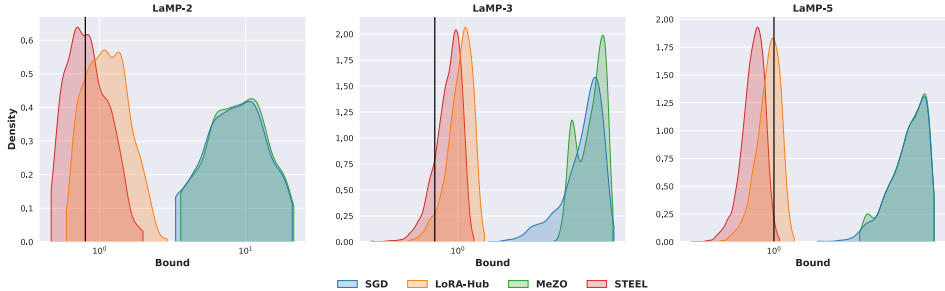


Figure 2: Distribution of generalisation guarantees (x-axis, log scale) obtained over few-shot LLM adaptation episodes. Vertical lines indicate the vacuous bound threshold. STEEL provides a dramatically better distribution of provable generalisation outcomes compared to alternatives.

Competitors: For single task methods that exploit only the foundation model and the target downstream task, we compare standard SGD, along with MeZO [17] and BBPT [38] – two state of the art gradient-free learners – for fine-tuning. For multi-task alternatives that exploit also the same task distribution as STEEL, we compare the model zoo learner LoRA-Hub [12] and the meta-learner MetaPB [39]. LoRA-Hub randomly samples from the model zoo and learns a new adapter as a linear combination of sampled adapters. Note that all methods are already combined with the same (experiment-specific) PEFT strategy for fair comparison. For SGD, MeZO, BBPT and MetaPB, this is an upgrade provided by us - they would definitely otherwise fail in the full parameter space. For SGD, MeZO, BBPT and LoRA-Hub, we combine them with recent quantization bound of [15] (Eq. 7) to provide guarantees, MetaPB uses their own PAC Bayes bound, and STEEL uses the bound in Eq. 3.

5.1 Guarantees for few-shot LLM adaptation

Datasets: For low-shot LLM adaptation, we use the LaMP personalization benchmark [24]. LaMP contains a fixed number of users per dataset that is split over training (seen) and evaluation (unseen) clients. Training and evaluation clients are mutually exclusive. Each client has their own support data and query data. We choose three datasets from the benchmark, namely LaMP-2 (Personalized Movie Tagging), LaMP-3 (Personalized Product Rating), and LaMP-5 (Personalized Scholarly Title Generation). These make nominal classification, ordinal classification, and text generation tasks respectively.

Setup: Following recent work on LaMP [30, 24], we first build a base model with task-specific capabilities by end-to-end fine-tuning of Flan-T5 base [4] on the user support data seen. Subsequently, to personalize the base model for a user, we train one LoRA-XS module on the support data of each training client [3]. LoRA-XS rank of 6 and an alpha of 16 was used, producing a total of 2592 tunable parameters. We build the model zoo by collecting the LoRA-XS modules trained using seen users support data; same data that was aggregated to finetune the base model. For computational efficiency, STEEL uses Hierarchical search as described in Section 3.4. We refer the reader to Appendix B.2 for detailed hyperparameters.

Table 1: LaMP LLM adaptation benchmark results.

	SGD	LoRA-Hub	MeZO	STEEL
LaMP-2	% Non-Vacuous Tasks	0.00%	<u>32.13%</u>	0.00% 65.12%
	Median Gap	8.12	<u>0.68</u>	8.45 0.43
	Min Bound	3.32	<u>0.59</u>	3.60 0.47
	Median Bound	8.52	<u>1.12</u>	8.85 0.80
	Max Bound	20.86	<u>2.90</u>	21.36 1.99
	Accuracy \uparrow	63.25%	<u>57.51%</u>	63.30% 63.74%
LaMP-3	F1 \uparrow	56.15%	50.84%	<u>57.03%</u> 55.69%
	% Non-Vacuous Tasks	0.00	<u>5.00</u>	0.00 15.48
	Median Gap	3.09	<u>0.23</u>	3.10 0.14
	Min Bound	1.35	<u>0.51</u>	2.54 0.43
	Median Bound	3.56	<u>1.04</u>	3.76 0.93
	Max Bound	4.75	<u>1.30</u>	4.53 1.17
	MAE \downarrow	0.217	<u>0.230</u>	0.242 0.231
LaMP-5	RMSE \downarrow	0.511	<u>0.526</u>	0.531 0.524
	Cross-Entropy \downarrow	0.479	0.739	<u>0.626</u> 0.693
	% Non-Vacuous Tasks	0.00	<u>63.84</u>	0.00 99.16
	Median Gap	4.04	<u>0.41</u>	4.04 0.26
LaMP-5	Min Bound	1.61	<u>0.52</u>	2.58 0.40
	Median Bound	4.57	<u>0.96</u>	4.57 0.81
	Max Bound	5.86	<u>1.25</u>	5.88 1.06
	ROUGE-1 \uparrow	47.04%	<u>47.05%</u>	47.03% 47.22%
	ROUGE-L \uparrow	42.79%	<u>42.75%</u>	42.73% 42.89%

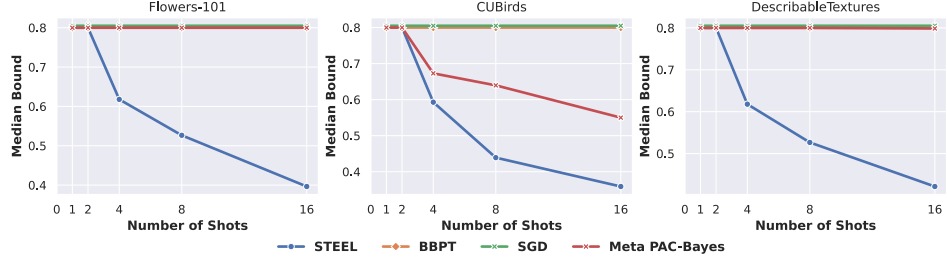


Figure 3: Dependence of generalisation guarantee on training set size. Our finite-hypothesis class learner STEEL achieves non-vacuous guarantees from 4-shot onward. Standard approaches provide no guarantees anywhere in this low-shot range.

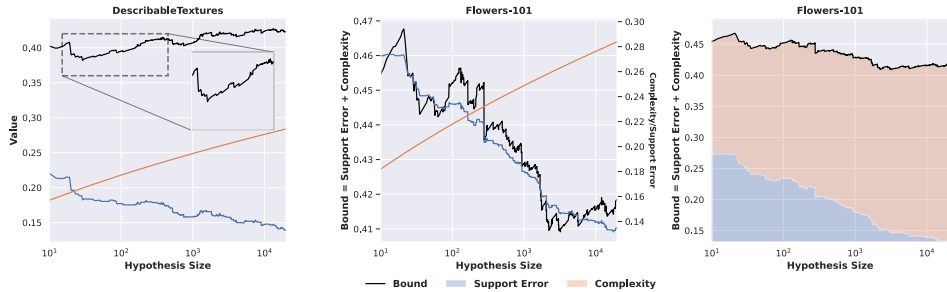


Figure 4: “Learning curves” illustrating empirical and certified learning dynamics of STEEL with respect to samples/iterations, which is equivalent to hypothesis space size. More samples improves the training (support) error, while increasing the complexity penalty. The sum of these two terms instantiates the generalisation guarantee (Eq. 3) achieved for a given number of samples.

Results: Our main contribution relates to the ability to provably certify the generalisation of low-shot learning. In terms of low-shot LLM adaptation, Figure 2 visualises the distribution of certification outcomes over a large number of episodes for the three LAMP benchmarks. Taking note of the log-scale on the x-axis for generalisation guarantee strength, we can see that our STEEL learner provides dramatically better guarantees than conventional continuous-parameter learner alternatives, thanks to its discrete hypothesis space. The vertical lines indicate the threshold for vacuous bounds. Standard learners such as SGD and MeZO have no mass left of the threshold, while a substantial number of STEEL learning episodes are non-vacuously guaranteed. Table 1 provides more detailed quantitative results in terms of various metrics. Notably, to assess provable generalisation, the data visualised in Figure 2 is summarised as the % non-vacuous metric (the fraction of episodes which have guarantees with a strength above chance-level), and the median guarantee strength across episodes.

From Table 1 results we can see that: (1) Standard supervised learning approaches such as (gradient-based) SGD and (gradient-free) MeZO have no non-vacuous episodes - no few-shot learning task can be guaranteed. (2) STEEL has the most non-vacuous episodes for each benchmark, with almost every few-shot learning episode being guaranteed in the LAMP-5 benchmarks. The median STEEL episode also has a substantially non-vacuous guarantee for all three benchmarks. (3) Interestingly, LoraHUB combined with Lotfi et al. [15]’s discretization bound also has some non-vacuous episodes, but less than STEEL. (3) STEEL has comparable or better empirical test accuracy compared to existing approaches such as SGD and MeZO, while providing a huge improvement in certifiability.

5.2 Guarantees for few-shot visual recognition

Datasets: For vision, we use fine-grained classification datasets that have readily available training (seen) and novel (unseen) classes split. We choose CUBirds [34], FGVC-Aircraft [16], Describable Textures [5] and Flowers-101 [20]. We use the split offered by learn2learn for the first three datasets [2], and the Flowers-101 split from Meta-Dataset [31].

Setup: We sample random few-shot n -shot k -way learning tasks as per meta-learning literature [31]. We use CLIP as our foundation model [22]. We randomly select 5 classes (5-way) from a given split

and for each class we randomly sample n -shots. We evaluate 1, 2, 4, 8 and 16-shots. The model zoo is built by sampling from the training classes of the aforementioned datasets. Meanwhile, we evaluate on unseen classes and samples. Please note that training and evaluation classes are mutually exclusive. For a given task, we use CoOp PEFT adaptation [41] which is simply prompt tuning for CLIP. We finetune a 2-token prompt appended in front of the class name for every task to build a model zoo. This results in total tunable parameters of length 1024. For vision experiments, we found that the forward passes were fast enough to conduct exhaustive search over sampled prompts from the diffusion model. For Meta-PB, we detail the meta-training setup, downstream adaptation and Meta-PB bounds in Appendix A.3. For details on all methods hyperparameters, we refer the reader to Appendix B.3.

Results: The results in terms of mean training and testing error versus complexity are summarised for three datasets in Figure 1. The dots for each learner reflect the training set sizes of 1, 2, 4, 8, and 16-examples per-class, and the white/grey zone separation delineates the space of non-vacuous vs vacuous bound outcomes. The main message is that only our finite hypothesis class approaches achieve any non-vacuous guarantees across this whole range of training set sizes. Every result for the standard SGD and BBPT approaches is vacuous and cannot be guaranteed. Please note, Meta-PB is not included as it is not directly comparable on the plot y-axis (empirical error term); Meta-PB uses the unbounded cross-entropy loss (Equation 23 as the risk metric, while our and other competing methods use empirical error.

For the 16-shot case, these experiments are quantified in Table 2. Similarly to the results for LLM adaptation, we can see the dramatic difference in % of non-vacuous episodes, and dramatic improvement in the min, median and max bound obtained over episodes. Compared to the LLM case, STEEL pays a slightly higher price in terms of empirical test accuracy compared to SGD for some benchmarks, however this is small compared to the stark difference in certification performance. The state of the art Meta-PB, also oriented at low-shot certification in some cases (CUB) manages to non-vacuously certify most episodes. However, in all cases the strength of this certification is much worse than STEEL (gap, median bound).

Figure 3 highlights the evolution of the median generalisation bound as a function of the training set size. For STEEL it becomes non-vacuous from 4-shots onward, and the standard approaches never become non-vacuous⁴

5.3 Further Analysis

Learning Curves: We discuss and provide some insight into the learning process of our discrete hypothesis class learner. Standard gradient-descent takes repeated update steps to find a model that better fits a training set. By analogy, our gradient-free STEEL draws more samples as it attempts to iteratively sample a model that better fits the training set. Our main experiments use a fixed number of 20,000 samples on all vision datasets. Figure 4 illustrates our learner’s behaviour by showing the equivalent of a learning curve for our model. The x-axis is the number of samples drawn, and equivalently the learning theoretic hypothesis space size. Unlike SGD, this means that there is a direct dependence of hypothesis class complexity ($|\Theta|$ in Eq. 3) and the number of iterations/samples. This is reflected in the steadily increasing red complexity curve in Figure 4(left, middle). We can also see that the training/support error goes down consistently over iterations/samples as the

Method	SGD	BBPT	Meta-PB	STEEL
CUBirds				
Non-Vacuous Ratio	0.00%	0.00%	97.50%	100.00%
Average Gap	2.49	2.48	0.45	0.24
Min Bound	2.55	2.55	0.34	0.30
Median Bound	2.58	2.59	0.55	0.36
Max Bound	2.64	2.68	0.85	0.47
Average Accuracy	90.32%	89.27%	89.24%	88.40%
Describable Textures				
Non-Vacuous Ratio	0.00%	0.00%	50.00%	100.00%
Average Gap	2.43	2.46	0.54	0.24
Min Bound	2.55	2.55	0.57	0.36
Median Bound	2.55	2.63	0.80	0.42
Max Bound	2.58	2.78	1.06	0.53
Average Accuracy	87.95%	83.20%	81.12%	81.50%
FGVCAircrafts				
Non-Vacuous Ratio	0.00%	0.00%	0.00%	97.50%
Average Gap	2.31	2.45	0.86	0.22
Min Bound	2.58	2.64	0.87	0.45
Median Bound	2.64	2.80	1.25	0.61
Max Bound	2.78	3.01	1.76	0.85
Average Accuracy	65.57%	62.37%	59.84%	61.37%
Flowers-101				
Non-Vacuous Ratio	0.00%	0.00%	10.00%	100.00%
Average Gap	2.51	2.50	0.68	0.27
Min Bound	2.55	2.55	0.65	0.31
Median Bound	2.55	2.59	1.15	0.40
Max Bound	2.55	2.70	1.77	0.61
Average Accuracy	95.90%	90.15%	71.23%	84.90%

Table 2: Few-shot visual recognition. Aggregate over 16-Shots 5-way learning episodes.

⁴Note their bound is substantially worse than 0.8, but for simple visualisation, we plot it as chance-level for 5-way classification.

sampler progressively discovers better models. The generalisation bound (black line) is given by the sum of the training error and complexity. The figure illustrates one case (Flowers, middle, right) where the bound continues to improve up to a large number of samples/hypothesis size, because the continued improvement in training error outweighs the complexity gain. It also illustrates a case (DTD, left) where the training error improvement is slower and quite rapidly outweighed by the complexity gain, so that the best bound is actually achieved after quite a small number of samples.

Sampler vs Zoo: Our approach compresses the upstream set of pre-trained models into a learned model generator. Selecting among the upstream models using downstream task performance as a criterion provides an alternative approach to learning that also corresponds to a finite hypothesis space. Our generator approach was motivated by ensuring scalability with respect to a large number of upstream models, and also to improve accuracy by enabling interpolation between upstream models rather than solely being limited to selecting one of them. Figure 1 shows that STEEL’s diffusion sampler tends to provide improved accuracy compared to its raw model zoo, especially for Flowers and DTD. On average across all datasets STEEL consistently outperforms Model Zoo. Detailed per-dataset per-shot performance is deferred to Appendix C, Table 3. Furthermore, we show in Appendix C.2 how to certify zero-shot CLIP using confidence intervals, and demonstrate that STEEL not only achieves tighter guarantees but also substantially outperforms it in terms of empirical performance.

Tightening STEEL Certificates: We focused thus far on the very low-shot regime to emphasise the unique achievement of obtaining the first non-vacuous certificate in this extreme setting. Nevertheless, stronger certificates may be necessary in many applications. We therefore explore increasing the training data from very low to moderately low shot. Specifically, we evaluate the iNaturalist dataset [9] (birds subset, with overlapping classes excluded) with a diffusion model pre-trained on CUB, which facilitates increasing shots to 128 examples. Results in Figure 5 show that: (1) As the training set grows, the support error increases initially as there are more data points to fit, but soon stabilizes. The finite hypothesis-space does not problematically under-fit an increasingly large training set. (2) Query error follows a similar trend, decreasing with support set size and saturating around 64 shots. (3) Crucially, the STEEL bound continues to improve with more shots. The increasing training set size continues to shrink the certificate’s complexity term, even after the support error has saturated, thus leading to continued tightening of the bound. At 64 or 128 shots, *the certified risk is tight – only 6% larger than the empirical test error*, while still using far fewer examples than standard certification approaches [15]. (4) This good result is obtained despite the distribution-shift (CUB vs iNaturalist) between upstream and downstream data. STEEL is robust to imperfect upstream-downstream task distribution alignment.

6 Conclusion

We have introduced a novel Sample-Then-Evaluate approach to transfer learning. Our STEEL is designed to facilitate non-trivial performance guarantees, even in the low-shot regime, through use of a discrete hypothesis space. Our results instantiating the bound demonstrate that for both LLM and visual transfer learning STEEL performs comparably to alternatives in terms of test accuracy, while being dramatically better in terms of ability to provably guarantee this performance level. Finally, based on our analysis from Section 5.3, we discuss future work in Appendix D.

References

- [1] P. Alquier. User-friendly introduction to PAC-Bayes bounds. *arXiv preprint arXiv:2110.11216*, 2021.
- [2] S. M. R. Arnold, P. Mahajan, D. Datta, I. Bunner, and K. S. Zarkias. learn2learn: A library for meta-learning research, 2020.
- [3] K. Bałazy, M. Banaei, K. Aberer, and J. Tabor. LoRA-XS: Low-rank adaptation with extremely small number of parameters, 2024.
- [4] H. W. Chung, L. Hou, S. Longpre, B. Zoph, Y. Tay, W. Fedus, Y. Li, X. Wang, M. Dehghani, S. Brahma, A. Webson, S. S. Gu, Z. Dai, M. Suzgun, X. Chen, A. Chowdhery, A. Castro-Ros, M. Pellat, K. Robinson, D. Valter, S. Narang, G. Mishra, A. Yu, V. Y. Zhao, Y. Huang, A. M. Dai, H. Yu, S. Petrov, E. H. Chi, J. Dean, J. Devlin, A. Roberts, D. Zhou, Q. V. Le, and J. Wei. Scaling instruction-finetuned language models. *J. Mach. Learn. Res.*, 2024.
- [5] M. Cimpoi, S. Maji, I. Kokkinos, S. Mohamed, , and A. Vedaldi. Describing textures in the wild. In *Proceedings of the IEEE Conf. on Computer Vision and Pattern Recognition (CVPR)*, 2014.
- [6] Y. Du, Z. Xiao, S. Liao, and C. Snoek. ProtoDiff: Learning to Learn Prototypical Networks by Task-Guided Diffusion. In *Advances in Neural Information Processing Systems*, 2023.
- [7] G. K. Dziugaite and D. M. Roy. Computing nonvacuous generalization bounds for deep (stochastic) neural networks with many more parameters than training data. *UAI*, 2017.
- [8] J. Ho, A. Jain, and P. Abbeel. Denoising Diffusion Probabilistic Models, 2020. In *Advances in Neural Information Processing Systems*.
- [9] G. V. Horn, O. M. Aodha, Y. Song, Y. Cui, C. Sun, A. Shepard, H. Adam, P. Perona, and S. Belongie. The inaturalist species classification and detection dataset, 2018.
- [10] T. M. Hospedales, A. Antoniou, P. Micaelli, and A. J. Storkey. Meta-Learning in Neural Networks: A Survey. *IEEE Transactions on Pattern Analysis and Machine Intelligence*, 2021.
- [11] E. J. Hu, Y. Shen, P. Wallis, Z. Allen-Zhu, Y. Li, S. Wang, L. Wang, and W. Chen. Lora: Low-rank adaptation of large language models. *arXiv preprint arXiv:2106.09685*, 2021.
- [12] C. Huang, Q. Liu, B. Y. Lin, T. Pang, C. Du, and M. Lin. Lorahub: Efficient cross-task generalization via dynamic LoRA composition. In *First Conference on Language Modeling*, 2024.
- [13] D. J. Koviczko, T. Blankevoort, and Y. M. Asano. VeRA: Vector-based Random Matrix Adaptation. In *International Conference on Learning Representations*, 2024.
- [14] J. Langford. Tutorial on practical prediction theory for classification. *Journal of Machine Learning Research*, 2005.
- [15] S. Lotfi, M. A. Finzi, Y. Kuang, T. G. J. Rudner, M. Goldblum, and A. G. Wilson. Non-vacuous generalization bounds for large language models. In *Forty-first International Conference on Machine Learning*, 2024.
- [16] S. Maji, J. Kannala, E. Rahtu, M. Blaschko, and A. Vedaldi. Fine-grained visual classification of aircraft. Technical report, 2013.
- [17] S. Malladi, T. Gao, E. Nichani, A. Damian, J. D. Lee, D. Chen, and S. Arora. Fine-tuning language models with just forward passes. In *Thirty-seventh Conference on Neural Information Processing Systems*, 2023.
- [18] M. Miranda, E. S. Ruzzetti, A. Santilli, F. M. Zanzotto, S. Bratières, and E. Rodolà. Preserving privacy in large language models: A survey on current threats and solutions, 2024.
- [19] M. Mohri, A. Rostamizadeh, and A. Talwalkar. *Foundations of Machine Learning*. MIT Press, 2018.

[20] M.-E. Nilsback and A. Zisserman. Automated flower classification over a large number of classes. In *2008 Sixth Indian Conference on Computer Vision, Graphics & Image Processing*, 2008.

[21] M. Perez-Ortiz, O. Rivasplata, J. Shawe-Taylor, and C. SzepesvÁri. Tighter risk certificates for neural networks. *Journal of Machine Learning Research*, 2021.

[22] A. Radford, J. W. Kim, C. Hallacy, A. Ramesh, G. Goh, S. Agarwal, G. Sastry, A. Askell, P. Mishkin, J. Clark, G. Krueger, and I. Sutskever. Learning transferable visual models from natural language supervision, 2021.

[23] F. Rezk, A. Antoniou, H. Gouk, and T. Hospedales. Liouna: Biologically plausible learning for efficient pre-training of transferrable deep models. In *2nd Workshop on Advancing Neural Network Training: Computational Efficiency, Scalability, and Resource Optimization (WANT@ICML 2024)*, 2024.

[24] A. Salemi, S. Mysore, M. Bendersky, and H. Zamani. Lamp: When large language models meet personalization, 2024.

[25] K. Schürholt, M. W. Mahoney, and D. Borth. Towards scalable and versatile weight space learning, 2024.

[26] S. Shalev-Shwartz and S. Ben-David. *Understanding machine learning: From theory to algorithms*. Cambridge university press, 2014.

[27] L. N. Smith and N. Topin. Super-convergence: Very fast training of neural networks using large learning rates, 2018.

[28] B. Soro, B. Andreis, H. Lee, W. Jeong, S. Chong, F. Hutter, and S. J. Hwang. Diffusion-based neural network weights generation. In *The Thirteenth International Conference on Learning Representations*, 2025.

[29] R. Staab, M. Vero, M. Balunovic, and M. Vechev. Beyond memorization: Violating privacy via inference with large language models. In *The Twelfth International Conference on Learning Representations*, 2024.

[30] Z. Tan, Z. Liu, and M. Jiang. Personalized pieces: Efficient personalized large language models through collaborative efforts. In *Proceedings of the 2024 Conference on Empirical Methods in Natural Language Processing*, 2024.

[31] E. Triantafillou, T. Zhu, V. Dumoulin, P. Lamblin, U. Evci, K. Xu, R. Goroshin, C. Gelada, K. Swersky, P.-A. Manzagol, and H. Larochelle. Meta-dataset: A dataset of datasets for learning to learn from few examples. In *International Conference on Learning Representations*, 2020.

[32] V. N. Vapnik. *The nature of statistical learning theory*. Springer-Verlag New York, Inc., 1995.

[33] R. A. Waelen. The ethics of computer vision: an overview in terms of power. *AI and Ethics*, 2023.

[34] C. Wah, S. Branson, P. Welinder, P. Perona, and S. Belongie. Cubirds dataset. Technical Report CNS-TR-2011-001, California Institute of Technology, 2011.

[35] K. Wang, D. Tang, B. Zeng, Y. Yin, Z. Xu, Y. Zhou, Z. Zang, T. Darrell, Z. Liu, and Y. You. Neural Network Diffusion. *arXiv preprint arXiv:2402.13144*, 2024.

[36] Y. Wang, Q. Yao, J. T. Kwok, and L. M. Ni. Generalizing from a few examples: A survey on few-shot learning. *ACM Comput. Surv.*, 2020.

[37] Y. You, J. Li, S. Reddi, J. Hseu, S. Kumar, S. Bhojanapalli, X. Song, J. Demmel, K. Keutzer, and C.-J. Hsieh. Large batch optimization for deep learning: Training bert in 76 minutes, 2020.

[38] L. Yu, Q. Chen, J. Lin, and L. He. Black-box prompt tuning for vision-language model as a service. In *Proceedings of the Thirty-Second International Joint Conference on Artificial Intelligence, IJCAI-23*. International Joint Conferences on Artificial Intelligence Organization, 2023.

- [39] H. Zakerinia, A. Behjati, and C. H. Lampert. More Flexible PAC-Bayesian Meta-Learning by Learning Learning Algorithms. In *International Conference on Machine Learning*, 2024.
- [40] B. Zhang, C. Luo, D. Yu, H. Lin, X. Li, Y. Ye, and B. Zhang. MetaDiff: Meta-Learning with Conditional Diffusion for Few-Shot Learning. 2024.
- [41] K. Zhou, J. Yang, C. C. Loy, and Z. Liu. Learning to prompt for vision-language models. *International Journal of Computer Vision (IJCV)*, 2022.

A Existing Risk Bounds for Deep Models

A.1 Vanilla PAC-Bayes Bound

This is the vanilla, non-transfer learning bound. As a baseline, one can also contrast with the vanilla PAC-Bayes bound (i.e., non-meta learning bound). This essentially follows the Canto’s bound, and can be written as follows. With probability at least $1 - \epsilon$, the following holds:

$$\mathbb{E}_{Q(\theta)}[R(\theta)] \leq \mathbb{E}_{Q(\theta)}[r(\theta)] + \sqrt{\frac{\text{KL}(Q||\pi) + \log(1/\epsilon)}{2n}} \quad (4)$$

Here n is the test support size. We can set $\pi = \mathcal{N}(0, \kappa^2 I)$ for some fixed κ_π and $Q(\theta) = \mathcal{N}(\mu, \Sigma^2)$ where the parameters (μ, Σ) can be learned by minimizing the right hand side. The sampled version $\theta^z = \mu + \sqrt{\Sigma} \cdot z$, $z \sim \mathcal{N}(0, I)$ can be used during the optimization. Once optimized, the minimum value of the right hand side serves as the error bound for the test task.

A.2 Bound with Parameter-Level Quantization

In [15], they proposed a non-vacuous bound for the LLM based on the model parameter quantization (e.g., fixed-length floating point machine representation). There are several differences to our approach:

1. The paper is about LLM pre-training setup with large training data, and the bound would be vacuous if training data size is not large enough (e.g., $\geq 10K$).
2. They derive the same finite hypothesis space PAC-Bayes bound, but replace the $\log |H|$ term by $\log(1/p(h))$ where $p(h)$ is the prior likelihood, and $\log(1/p(h))$ is approximated and upper-bounded by $C(h)$ which is the number of bits for representing the hypothesis h .
3. The finite hypothesis space comes from the fixed-size floating point representation for real numbers (e.g., if there are d trainable parameters, then $C(h) = d \cdot 32$), but to reduce it further, they propose what is called the SubLoRA, which is a random subspace representation (i.e., $\theta = Pw$, P = random subspace basis, w = coefficients) of the LoRA A/B matrices.
4. Also, instead of 32 bit for each of d params, they do some clustering to reduce it to shorter coding, more precisely the arithmetic coding.

The followings are some details of their bound derivation. With probability at least $1 - \epsilon$,

$$R(\theta) \leq r(\theta) + C \cdot \sqrt{\frac{K(\theta) + 2 \log K(\theta) + \log(1/\epsilon)}{2n}} \quad (5)$$

where $K(\theta)$ is the Kolmogorov complexity bound that can be estimated as:

$$K(\theta) = \sum_{i=1}^d (\# \text{ of bits in the arithmetic coding of } \theta_i) \quad (6)$$

where $d = \dim(\theta)$ for the PEFT parameters θ . The arithmetic coding requires clustering of parameters θ_i s, thus being dependent on the particular θ used. However, we can consider the best (i.e., the tightest) bound possible. That is, even if we have 1 bit for every θ_i (the minimal code length possible), $K(\theta) = d$, and plugging this into (5) yields:

$$R(\theta) \leq r(\theta) + C \cdot \sqrt{\frac{d + 2 \log d + \log(1/\epsilon)}{2n}} \quad (7)$$

which is the *best* scenario.

In (5), as before, $R(\theta) = \mathbb{E}_{z \sim T^*}[l(\theta; z)]$ is the generalization error of θ , $r(\theta) = \frac{1}{n} \sum_{z \in S^*} l(\theta; z)$ is the empirical error on the support data with size $n = |S^*|$, and C is the maximal loss value (i.e., $0 \leq l \leq C$).

A.3 PAC-Bayes Meta Learning Bound

In [39] they proposed an extension of the PAC-Bayes bound for meta learning. Their meta learning algorithm aims to learn a distribution over the adaptation algorithms $A(S) \rightarrow Q(\theta)$ where S is the support training data for a task and $Q(\theta)$ is the posterior distribution in the PAC-Bayes theorem. In their paper, any adaptation algorithm A is allowable provided that A internally makes use of a prior distributions in the PAC-Bayes theorem (e.g., the adaptation algorithms that try to minimize the PAC-Bayes bound), so that $A(S)$ becomes a function of the prior. And the meta learning model is a distribution ρ that can sample the prior, and the meta learning amounts to learning the distribution ρ .

Although they provided a concrete example in Appendix B.2 in their paper, the described meta training involves an optimization of a loss function that contains an optimal value of another problem, which is typically attained by gradient descent. Just like MAML-type algorithms with a large number of inner gradient steps, this renders the application of their theorem to large-scale model/data impractical. So we propose a more practical reptile-like adaptation strategy, essentially admitting a closed-form inner optimal solution, that is practical in large model/data scenarios. Note that under our setting the meta learning PAC-Bayes bound is still applicable since they said the theorem works for *any* adaptation algorithms.

A.3.1 Concrete Cases with (Reptile-Like) Quadratic-Regularized Adaptation Algorithms

Let θ be the parameters of a neural network or PEFT parameters. Denote $\dim(\theta)$ by d . The adaptation algorithm $A(S)$ returns a PAC-Bayes posterior $Q(\theta) = \mathcal{N}(\mu, \Sigma)$ for some task support data S as input. We consider diagonal Σ . The algorithm A itself is parametrized by the PAC-Bayes prior $P_1(\theta) = \mathcal{N}(\mu_1, \Sigma_1)$ since we only deal with those A s that internally use P_1 as a part of the algorithm without dependency on any other things. One candidate for A is the algorithm that minimizes the PAC-Bayes bound with prior P_1 with respect to $Q(\theta)$. However, as said earlier, this incurs MAML-like optimization that is impractical.

Our choice of A is as follows: (Step-1) We first find $(\mu^{SGD}, \Sigma^{SGD}) = \arg \min_{\mathcal{N}(\theta; \mu, \Sigma)} \mathbb{E}[l(\theta; S)]$ by gradient descent. Technically, this involves evaluating $l(\theta; S)$ with reparametrized $\theta = \mu + \sqrt{\Sigma}z$ for $z \sim \mathcal{N}(0, I)$, where the gradients take: $\nabla_\mu l(\theta; S) = \nabla_\theta l(\theta; S)$ and $\nabla_\Sigma l(\theta; S) = \nabla_\theta l(\theta; S) \cdot 0.5\Sigma^{-0.5}z$ by the chain rule. So it is as tractable as SGD since we only need conventional backprop $\nabla_\theta l(\theta; S)$ to get gradients with respect to (μ, Σ) . (Step-2) Solve the following quadratic optimization:

$$(\mu^*, \Sigma^*) = \arg \min_{\mu, \Sigma} \|(\mu, \Sigma) - (\mu^{SGD}, \Sigma^{SGD})\|^2 + \alpha \cdot \|(\mu, \Sigma) - (\mu_1, \Sigma_1)\|^2 \quad (8)$$

The intuition is that the adapted model (μ, Σ) has to be close to the fitted $(\mu^{SGD}, \Sigma^{SGD})$ and also close to the prior (μ_1, Σ_1) . The trade-off coefficient α is user's choice, but when inspired by the PAC-Bayes bound objective, we can set $\alpha = 1/\sqrt{|S|}$. The main benefit of this quadratic-regularized adaptation algorithm is that we have the closed-form solution:

$$\mu^*(\mu_1, S) = \frac{1}{1+\alpha} \mu^{SGD} + \frac{\alpha}{1+\alpha} \mu_1 \quad (9)$$

$$\Sigma^*(\Sigma_1, S) = \frac{1}{1+\alpha} \Sigma^{SGD} + \frac{\alpha}{1+\alpha} \Sigma_1 \quad (10)$$

Note that (μ^*, Σ^*) are functions of the prior (μ_1, Σ_1) , and so we used the function notation in (9–10) together with dependency on S although μ^* does not depend on Σ_1 and Σ^* similarly. We treat $(\mu^{SGD}, \Sigma^{SGD})$ as constant.

Next we define the meta prior (π) and posterior (ρ) distributions for the meta learning PAC-Bayes bound. As suggested in [39],

$$\pi(A) = \mathcal{N}((\mu_1, \Sigma_1); 0, \kappa_\pi^2 I_{2d}) \quad (11)$$

$$\rho(A) = \mathcal{N}((\mu_1, \Sigma_1); M_1, \kappa_\rho^2 I_{2d}) \quad (12)$$

where $M_1 = (M_1^\mu, M_1^\Sigma)$ is the parameters for the meta posterior ρ . Here κ_π and κ_ρ are the fixed scales, and in their paper they used $\kappa_\pi = 100$ and $\kappa_\rho = 10^{-3}$. Finally, they assume delta meta prior and posterior in the complexity term: $\mathbb{P}(A) = \mathbb{Q}(A) = \delta_{P_1}$.

This leads to the following meta training objective:

$$\min_{M_1} \hat{R}(\rho) + \underbrace{\sqrt{\frac{\text{KL}(\rho||\pi) + \log(4\sqrt{N}/\epsilon)}{2N}}}_{=:T_1} + \underbrace{\sqrt{\frac{\text{KL}(\rho||\pi) + N\hat{E}(\rho) + \log(8nN/\epsilon) + 1}{2nN}}}_{=:T_2} \quad (13)$$

where

$$\hat{R}(\rho) = \mathbb{E}_{A \sim \rho} \left[\frac{1}{N} \sum_{i=1}^N l(A(S_i); S_i) \right] \quad (14)$$

$$\hat{E}(\rho) = \mathbb{E}_{A \sim \rho} \left[\frac{1}{N} \sum_{i=1}^N \text{KL}(A(S_i) || P_1) \right] \quad (15)$$

$$\text{KL}(\rho||\pi) = \frac{2d\kappa_\rho^2 + \|M_1\|^2}{2\kappa_\pi^2} - d + 2d \log \frac{\kappa_\pi}{\kappa_\rho} \quad (16)$$

Recall that n is the support data size and N is the number of meta training tasks.

Meta training procedure (stochastic approximation version). Since it is nearly infeasible to compute the objective for all N tasks (for the purpose of one gradient update for M_1), we adopt the stochastic approximate optimization. That is, for each sampled task batch B (out of N tasks), we compute the followings (stochastic estimates of the objective and the gradient):

- $\hat{T}_0 \approx \hat{R}(\rho)$ where

$$\hat{T}_0 = \frac{1}{|B|} \sum_{i \in B} l(\theta^{z_i}; S_i), \quad (17)$$

$$\theta^{z_i} = \mu^*(\mu_1, S_i) + \sqrt{\Sigma^*(\Sigma_1, S_i)} \cdot z_i, \quad z_i \sim \mathcal{N}(0, I_d) \quad (18)$$

$$\mu_1 = M_1^\mu + \kappa_\rho \cdot z^\mu, \quad z^\mu \sim \mathcal{N}(0, I_d) \quad (19)$$

$$\Sigma_1 = M_1^\Sigma + \kappa_\rho \cdot z^\Sigma, \quad z^\Sigma \sim \mathcal{N}(0, I_d) \quad (20)$$

Here $\mu^*(\mu_1, S_i)$ and $\Sigma^*(\mu_1, S_i)$ are determined by (9–10). Note that \hat{T}_0 is a function of M_1 , and the gradient of \hat{T}_0 with respect to M_1 can be obtained from $\nabla_{\theta^z} \hat{T}_0$ by the chain rule similarly as described previously.

- T_1 as it is since it is easy closed-form.
- $\hat{T}_2 \approx T_2$ where \hat{T}_2 only replaces $\hat{E}(\rho)$ by the following from T_2 :

$$\hat{E}(\rho) \rightarrow \frac{1}{|B|} \sum_{i \in B} \text{KL}(A(S_i) || P_1) \quad (21)$$

$$= \frac{1}{|B|} \sum_{i \in B} \text{KL}(\mathcal{N}(\mu^*, \Sigma^*) || \mathcal{N}(\mu_1, \Sigma_1)) \quad (22)$$

This has a closed form from the Gaussian KL formula.

As the above steps allow us to compute the meta training objective and its gradient, we can update M_1 , and move on to a next batch.

Test-time bound. Once we have meta-learned M_1 , we can compute the error bound for a new task that comes with the support data S^* . In essence, we solve the following optimization problem:

$$Q^* = \arg \min_Q \hat{R}(Q) + \sqrt{\frac{\text{KL}(Q||P_1) + \log(8n/\epsilon) + 1}{2n}} \quad (23)$$

We parametrize $Q = \mathcal{N}(\mu, \Sigma)$ and solve it with respect to (μ, Σ) . First, $\hat{R}(Q)$ can be approximated by $l(\theta^z; S^*)$ with $\theta^z = \mu + \sqrt{\Sigma} \cdot z$, $z \sim \mathcal{N}(0, I_d)$. We can use the chain rule similarly for $\nabla_{\mu, \Sigma} \hat{R}(Q)$. In the KL term, P_1 has to be sampled from ρ (i.e., our learned M_1). We can use $P_1 = \mathcal{N}(M_1^\mu + \kappa_\rho \cdot z^\mu, M_1^\Sigma + \kappa_\rho \cdot z^\Sigma)$ and compute the KL using the Gaussian KL formula. Once optimized, the minimum value of (23) becomes the error bound for this test task which holds with probability at least $1 - \epsilon$.

B Architecture and Training Recipes

B.1 Diffusion Architecture and Training Recipe

First, the diffusion model forward encoder uses a 1000 timesteps with a linear scheduler over noise between $1e-4$ to $2e-2$. For the decoder, we use an MLP network for the diffusion model with 3 hidden-layers. The hidden layer dimension is $4 \times$ the size of its input. This is 10,240 for LaMP (divisible by 512 for parallelization concerns) and 4096 for vision. A layer conditioned time embedding of the diffusion step is added (summed with) the hidden layer’s hidden representation.

The time embedding is generated from the diffusion timestep using sinusoidal embeddings as per the original DDPM model [8]. The dimensionality of the sinusoidal embedding is equal to the Diffusion MLP hidden dimension. Subsequently, the embedding is transformed using a two-layer MLP with first layer expanding the dimension to $4 \times$ the network’s hidden dimension and the second layer downscaling again to original hidden dimension. For example, on the vision experiments, the time embedding network has hidden dimension of 4098×4 . Finally, to condition the time embedding computed by the two-layer MLP time embedding network for each layer, we apply a different linear transformation per diffusion hidden layer.

We train the diffusion model for 30K epochs for all experiments with a batch size of 1,024. We use the LAMB optimizer [37] with a learning rate of 0.01. For vision experiments, we found that we can continue improving performance if we continue training for a second stage of 10K more epochs. For the second stage, we use a one-cycle learning rate scheduler [27] with default hyperparameters (as found in pytorch). The maximum learning rate starts from 0.0004 reaching a maximum of 0.001 over a 1000 steps. We keep an exponential-moving average of the network weights throughout training with a decaying rate of 0.9999.

B.2 Flan-T5 + LaMP Hyperparameters

For training the base model across all datasets, we use LaMP’s original recipe [24]. We use a batch size of 64, AdamW optimizer with a learning rate of $5e-5$ and weight decay of size 0.0001. We use a linear warmup for the learning rate over 5% of the total number of training steps.

To build the model zoo, we found that we required to tune Adam optimizer learning rate and per-dataset epochs per-dataset. We optimizer the hyperparameters to improve performance on the training split (seen users) query data. We use learning rates of 0.01, 0.01, 0.0001 and 20, 10, 10 epochs for LaMP-2, LaMP-3 and LaMP-5 respectively. For all datasets, we used a linear warmup for the learning rate over 5% of the total number of training steps. We used the same recipe to train a per-user LoRA-XS model on the unseen users/novel tasks.

For LoRA-Hub, we used default hyperparameters as proposed by the original authors. First, we sample 20 random adapters from the model zoo. The weights of the linear combination is initialized with zeros and truncate min/max weights to $-1.5/1.5$. We do maximum inference steps of 40 with NeverGrad default hyperparameters.

Finally, we transform the SGD number of epochs to MeZO. The authors used $32 \times$ as many epochs as SGD in the original paper [17]. This translates to 640, 320, 320 epochs for LaMP-2, LaMP-3, and LaMP-5. We tested the three learning rates proposed to search over by the authors. We fixed a learning rate of $1e-3$ across all datasets because we consistently found $1e-4$ to not learn and $1e-2$ to be unstable.

For LaMP, we sample 10K LoRA-XS modules from the diffusion model. We use k-means clustering on the diffusion samples to produce N clusters where N is chosen as the minimum Silhouette score. We evaluate N between [2,150] inclusive. For each cluster, we find the medoid; the adapter closest to the centroid of the cluster. During evaluation, we choose a cluster and evaluate all adapters therein. From the cluster, we short-list the best 15 adapters using the Flan-T5 training loss. On the best 15 adapters, we use text generation to produce an answer with greedy sampling. Using the LaMP benchmark proposed model selection metric for each dataset, we select the “winning” adapter.

B.2.1 Bound Metrics

For support errors, we use 1-Accuracy for LaMP-2, and ROUGE-1 for LaMP-5. For LaMP-3, both RMSE and MAE are not bounded. Therefore, we devise a cross-entropy like metric for the dataset. First, we convert the ordinal vectors to one-hot encodings. Subsequently, we calculate the absolute error between the labels one-hot encoding and Flan-T5 model logits, and divide by 2. This guarantees the error to be bounded in the [0-1] range inclusive. We use this metric as support error term.

LaMP-2 Intricacies: LaMP benchmark has one query sample per user. For LaMP-3 and LaMP-5, this suffices since the generated support error is continuous. Nevertheless, for LaMP-2, the accuracy term, which we use to derive the support error, becomes the 0/1 loss. Therefore, we split the support data in novel tasks to support and query data with ratio 80% and 20% respectively. If the split generates only 1 query samples, we move one sample from support to query to have a minimum of two-samples in query. We use the same split for all evaluations across SGD, MeZO, LoRA-Hub and our proposed methods. For reproducibility, all splits were done deterministically. Furthermore, we did not constrain the split to have same classes across both support and query. LaMP classification tasks are long-tailed. Therefore, for a novel task, a user might have classes X and Y in support but the query ends up with classes A and B making it a more challenging benchmark for all methods.

Finally, we truncate the support sizes of LaMP-3 and LaMP-5 to 256 samples across all methods. This is done deterministically for reproducibility. The reason for truncating the dataset is pure computational concerns.

B.2.2 Model Zoo Size

For LaMP, we build a model zoo by training one PEFT adapter per-task in the dataset. Each user is treated as one task. This yields 3820, 20,000, and 9,682 total adapters/tasks in LaMP-2, LaMP-3, and LaMP-5 respectively.

B.2.3 Compute Resources

All experiments were conducted on 10xA40 GPUs. The base model finetuning for generating task specific models took a couple of hours with a batch size of 64 using 2 GPUs. Time to train an adapter for one user using one GPUs varies from dataset to dataset and from user to user depending on their available dataset size. This takes as low as 10 seconds and up to 2 mins per user. Diffusion model training on the collected model zoo varied among datasets too since each epoch was of different total number of steps because of different dataset sizes. We used one A40 GPU per diffusion model and train using the recipe described earlier. Finally, downstream adaptation using STEEL varies between datasets. For LaMP-2, this was 50 A40 GPU hours and LaMP-5 was the slowest with 1200 A40 GPU hour since it requires text generation.

B.3 CLIP + CoOP Hyperparameters

To build the model zoo, we used the authors original hyperparameters to train CoOP because we found them to work the best. This is SGD with a learning rate of 0.002. For Flowers-101, we train for 200 epochs. For DTD, FGVC-Aircraft and CUBirds, we trained for 300 epochs and found a One Cycle learning rate useful to stabilize training. These same hyperparameters were used to evaluate SGD on novel tasks. For BBPT, we use the authors default hyperparameters [38]. We found that the method converges within 8000 “API call”. We attempted to run for a budget of 20K as our diffusion model offers but found that performance did not improve. Please note that the original authors reduce the dimensionality of the prompt using a small network because evolutionary optimization struggles in high-dimension. They reduce dimensionality to 512. Nevertheless, since we train only 2-tokens (dimensionality=1,024), then we do not use the small dimensionality reduction network.

Finally, for MetaPB, we train the upstream model for 20 epochs on our model zoo which takes 24 hours similarly to our diffusion model training. We use Adam with default learning rate of 0.01 for both upstream and downstream. Downstream adaptation was done for 300 epochs with same Adam optimizer setting. We train both means and variances. Variances are clipped to 0.1 for numerical stability.

For vision experiments, we found that exhaustive search was fast enough even though we sample 20K adapters from the diffusion model.

Bound Metrics: we use $1 - \text{Accuracy}$ as the support error term in our bound calculation for all vision experiments.

Model Zoo Size: We randomly sample 16-shot 5-way tasks for building the model zoo from each respective dataset. We train 10,000 total tasks per-dataset for the model zoo. The diffusion model is trained on this model zoo. Once trained, we sample the diffusion model once and fix the samples across all downstream evaluation for 1, 2, 4, 8 and 16 shots.

Compute Resources: For SGD, training one task upstream for model zoo collection or downstream for gradient descent adaptation takes 10-15 seconds. BBPT downstream takes 10-15 seconds as well. Training the diffusion model on a model zoo, since we fix model zoo size in CLIP experiments, was the same among all experiments. Each diffusion model took 24 A40 GPU hours to train. STEEL takes 30 second to 1 minute downstream for adapting to a new task. Finally, meta-training phase of MetaPB takes 24 hours similarly to our diffusion model training. MetaPB downstream takes 15 second per task too.

C Extra Vision Results

C.1 Accuracy Results Across Shots

Dataset	Zero Shot	SGD	BBPT	Meta-PB	Model Zoo	STEEL
1-Shots						
CUBirds	83.82%	81.77%	85.80%	88.25%	86.00%	86.72%
DescribableTextures	67.29%	69.97%	74.10%	78.55%	72.12%	73.97%
FGVCAircraft	47.44%	53.00%	55.05%	56.46%	54.37%	55.40%
Flowers-101	81.14%	83.55%	80.40%	54.20%	74.25%	76.75%
Avg	69.92%	72.07%	73.84%	69.37%	71.69%	73.21%
2-Shots						
CUBirds	83.82	85.82%	86.92%	88.40%	86.77%	86.50%
DescribableTextures	67.29	75.95%	76.57%	78.99%	75.22%	76.17%
FGVCAircrafts	47.44	52.30%	57.90%	58.31%	55.82%	57.30%
Flowers-101	81.14	86.92%	85.05%	61.25%	77.17%	79.50%
Avg	69.92	75.25%	76.61%	71.74%	73.75%	74.87%
4-Shots						
CUBirds	83.82	88.30%	88.42%	88.77%	87.50%	87.47%
DescribableTextures	67.29	81.02%	77.90%	78.85%	77.40%	79.82%
FGVCAircrafts	47.44	58.65%	60.55%	58.26%	57.55%	60.10%
Flowers-101	81.14	91.95%	87.07%	65.44%	79.82%	81.42%
Avg	69.92%	79.98%	78.49%	72.83%	75.57%	77.21%
8-Shots						
CUBirds	83.82	89.75%	88.40%	88.68%	87.42%	87.32%
DescribableTextures	67.29	85.07%	81.47%	79.96%	79.90%	81.77%
FGVCAircrafts	47.44	62.07%	61.55%	58.56%	58.77%	61.72%
Flowers-101	81.14	94.30%	88.67%	68.72%	80.32%	82.52%
Avg	69.92%	82.80%	80.02%	73.98%	76.61%	78.34%
16-Shots						
CUBirds	83.82	90.32%	89.27%	89.24%	87.97%	88.40%
DescribableTextures	67.29	87.95%	83.20%	81.12%	79.25%	81.50%
FGVCAircrafts	47.44	65.57%	62.37%	59.84%	61.02%	61.37%
Flowers-101	81.14	95.90%	90.15%	71.23%	82.92%	84.90%
Avg	69.92%	84.94%	81.25%	75.36%	77.79%	79.04%

Table 3: CLIP+CoOp few-shot learning. Accuracies over different number of shots.

C.2 Certifying Zero-Shot Performance

Median Bound	Flowers	CUB	DTD	FGVVCA
STEEL	0.40 (+0.03)	0.36 (-0.06)	0.42 (+0.11)	0.61 (+0.10)
ZS CLIP	0.43	0.30	0.53	0.71

Table 4: Comparing median bounds between STEEL and zero-shot CLIP given a 16-shots support set.

One might assume that zero-shot CLIP is a strong *certified* baseline because it is evaluated without any fine-tuning, and the support and query sets are drawn i.i.d. from the same distribution. This can lead to the impression that its support-set accuracy reflects test-time performance. However, these are still empirical estimates and do not account for uncertainty due to sampling. In contrast, our certificates explicitly bound the generalization gap from limited support data. To facilitate a fairer comparison, we compute a Langford-style test-set bound (Theorem 3.3 by Langford [14]) using zero-shot CLIP’s support accuracy from Table 3, treating it as a proxy for true performance. The resulting guarantees are included in the table below. While zero-shot CLIP performs well empirically, our STEEL method achieves tighter guarantees and often stronger accuracy in the few-shot setting.

D Limitations and Future Work

As discussed in the main paper (see Section 5.3), increasing support set size continues to tighten the certificate without causing underfitting. Beyond this, there remain several promising directions for further improving certificate strength. One avenue is to refine the structure of the hypothesis class. The current bound treats hypotheses as independent, but in practice, many may yield highly correlated predictions. Accounting for this redundancy, for instance, by discounting the contribution of similar models, could lead to tighter bounds. Another opportunity lies in the use of hybrid hypothesis classes. For example, treating each sample as a mean of a Gaussian mixture component and applying PAC-Bayesian fine-tuning may yield posterior distributions that better fit the data while maintaining low complexity. These strategies suggest that the certification framework presented here can be further enhanced by incorporating richer modeling and more expressive prior structures.

E Broader Impact

This paper presents work whose goal is to advance the field of Machine Learning. There are many potential societal consequences of our work, and we mention a non-exhaustive concerns here. First, for LLM experiments, please note that the diffusion model is trained on adapters trained on user-specific data. We can use the diffusion model to interpolate between adapters to potentially avoid distributing the private model zoo among clients, but this does have potential for data leakage by memorization [29]. It is worth investigating privacy preserving methods for such concerns [18].

On the vision side of our experiments, despite our benchmark being on fine-grained classification tasks of publicly available datasets, we necessitate the reminder of ethical concerns in computer vision as our method is easily applicable across domains and applications [33].